

OPTIMIZATION OF BROADBAND MICROWAVE ABSORBER USING GENETIC ALGORITHM

Pham Van Hai, Vu Minh Tu, Mai Ngoc Van, Pham Van Dien
and Tran Manh Cuong

Faculty of Physics, Hanoi National University of Education

Abstract. In recent years, scientists have been focusing on coding metamaterials absorbers to take full advantage of digital technology. This technology is mostly based on the fact that the absorption spectrum of a full-sized metamaterial varies with the different number and position of the defect elements in conventional unit cells (UCs) in it. However, both of their traditional methods namely simple random sample and combination of fundamental meta-block struggle with the enormous number of possible configurations especially when the number of UCs increases. In this article, we represent 5 configurations with different numbers of UCs, 2x2, 3x3, 4x4, 5x5, and 6x6 UCs, all of which maintain average absorption higher than 90% over a 10 GHz wide frequency range of interest between 17 GHz and 27 GHz. These results are obtained by using a genetic algorithm to generate configurations with higher optical loss through the process. Comparing to the conventional methods' result, our approach has achieved a significant improvement in the absorption spectrum. Furthermore, our methods could be applied to more structures with different sizes and numbers of UCs, thus provided a reliable tool to design practical metamaterials that serve the real work demands.

Keywords: metamaterials, genetic algorithm broadband absorption.

1. Introduction

For the last few decades, scientists have been focusing on optimizing the absorption spectrum of electromagnetic absorber because of its wide range of applications in emissivity control [1, 2-4], superlens [5-7], solar cell enhancement [8, 9], spectroscopy [10, 11], and thermal imaging [1, 12, 13]. One of their recent and advanced solutions is metamaterials.

A metamaterial is an artificial material that is an assembly of periodic metal circuits in a dielectric substrate. It was predicted theoretically for the first time by Veselago, a Soviet/Russian physicist, in 1968 [14]. However, it took the scientists almost four decades to realize the preeminent properties of this material, especially after Landy et al. proposed

Received June 12, 2020. Revised June 23, 2020. Accepted June 29, 2020.

Contact Pham Van Hai, e-mail address: haipv@hnue.edu.vn

the first demonstration of metamaterial perfect absorber (MPA) in 2008 [6, 15].

An innovative idea based on control defects was introduced to overcome the electromagnetic absorbers' common drawbacks namely the requirement of complex configuration and optimization. Since the working principle of electromagnetic absorbers is based on the conversion of an electromagnetic wave into heat caused by the electric or magnetic losses in the constituent, controlling the number of optimal unit cells and manipulating the defect's location will enable us to create a broadband MPA [16].

A variety of methods namely: all-metal or all-dielectric structure, multilayered, asymmetric, super-cell structure, and hybrid structure have been demonstrated with positive results [17-29], however, they are still held back by the high complexity and low flexibility and hence have poorly realistic applications. Hence, several researchers have chosen to approach with digital or coding metamaterial absorber to enhance the applicability and take full advantage of digital technology.

There are two main traditional ways to approach with coding metamaterial absorber that are simple random sample (SRS) method and combination of fundamental meta-block (CFM) [16]. However, these two methods both struggle with the enormous statistical population especially when the number of basic unit cells in the configurations increases. Hence, in this study, we focus on optimizing the configurations of the full-sized structure metamaterials by using a genetic algorithm and compare the result's absorption spectrum to those obtained by two previous methods in Ref. [16].

2. Content

2.1. Model and simulation methods

2.1.1. Model

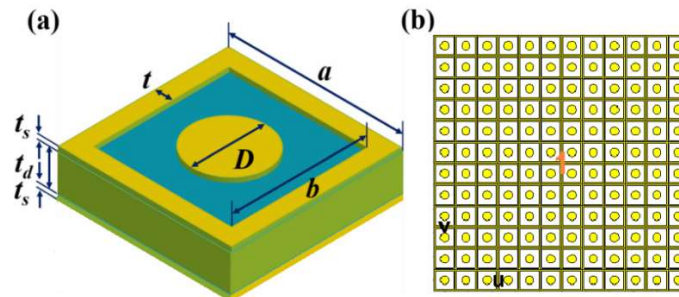


Figure 1. (a) An elementary unit cell with structural parameters, (b) a full-sized 12x12 UCs structure.

Reprinted with permission from Manh Cuong Tran et al, Scientific Reports 10 (2020) 1810. Copyright Springer Nature

A full-sized metamaterial is constructed by a certain number of Unit cell (UC). Figure 1 illustrates the 3D structure of a UC with its parameters. As can be seen from the image, the cell consists of a layer of FR-4 (lossy) dielectric and two layers of copper. The bottom layer having the thickness of $t_s = 0.03mm$ is completely covered by copper which is modeled as a lossy metal with an electric conductivity of $\sigma = 5.82 \times 10^7 S/m$. An FR-

4 dielectric substrate having a dielectric constant of 4.3 and a loss-tangent of 0.025 is used to form the middle layer. FR-4 is a glass-reinforced epoxy laminate material which is a material composed of woven fiberglass cloth with an epoxy resin binder having the self-extinguishing property. It is used in this model because of its ability to maintain its high electrical insulating in different conditions (e.g. dry or humid) as well as its excellent fabrication property. The thickness of the middle layer is $t_d = 1.5mm$. Lastly, a square ring, whose outer and inner side lengths are $a = 9mm$ and $b = 7.8mm$ respectively (meaning its width is $t = \frac{a-b}{2} = 0.6mm$), surrounds a dish which is 3.5 mm in diameter (D) is placed on top of the structure to complete the metamaterial. Both are made of copper which has the exact same thickness (t_s) and electric conductivity (σ) as the bottom layer. This design is chosen because it is simple and easy to control the working frequency range by rescaling its parameters [30].

2.1.2. Simulation method

Regarding the simulation tool, CST Microwave studio based on the Finite Integration Technique (FIT) is used to simulate the wave-matter interaction [16]. In this study, the boundary conditions are set to be open. Additionally, the electromagnetic wave is orient to be incident normally on the surface thanks to the waveguide port placed in front of the structure. Because the bottom of the configuration is a thick layer of copper, the wave is completely reflected into the material after it passes through the dielectric layer. Thus, there is no transmittance and the absorptivity is the difference between unity and the reflectance.

Our program in MATLAB instructs the commercial simulator CST Studio Suite to construct various configurations by generating two-dimensional logic $n \times n$ matrices. Here, “1” is the UC with a metal plate, “0” is the UC without a metal plate. CST Studio Suite will then add a waveguide and perform the simulation. After that, the magnitude of S_{11} parameters is collected and used to calculate the absorption to analyze in the future.

2.1.3. Optimization process

We use a genetic algorithm (GA) to optimize the structure. These algorithms were mostly inspired by natural selection, the key mechanism of biological evolution. It constantly modifies a selected or random population of different solutions. Through each step, individuals are paired up to be parents and produce the next generation. However, the process is not random but the selection operator chooses which “chromosomes” (e.g., strings of “bits”) in the population to be reproduced in the next generation. Normally, the fitter chromosomes will produce more offsprings. After the process of reproduction and selection, the population advance to an optimal solution.

There are three major rules for the GA to produce new generation from the current population:

- Selection rules choose the individuals to pair up to contribute to the population at the next generation.
- Crossover rules combine two parents to form children for the next generation.
- Mutation rules apply random changes to individual parents to form children.

In our study, the “chromosomes” were chosen based on target properties which are their reflectances and transmittances at a set of test frequencies. Thanks to the thick

copper layers at the bottom of the structures that the transmittance is zero and the reflectance is the difference between unity and the absorption. Hence the reflectance of the structures is calculated through the following cost function:

$$\text{cost} = \sum_{f=f_1}^{f=f_2} 1.0 - A_{(f)}^2 \quad (1)$$

where $A_{(f)}$ is the transverse absorptivity measured corresponding to each frequency, f_1 and f_2 is the frequency of interest. The metamaterial configurations are evolved to have ideal absorption spectra over the test wavelengths by the GA as it minimizes the cost function in Equation (1).

2.2. Result and discussion

To verify the working frequency of the configuration for further investigation, various simulations of 4, 16, 64, and 100 UCs metamaterial have been performed and their absorption spectra are shown in Figure 2. It is clear that the high absorption range of structures is in a range from 17 GHz to 27 GHz. Therefore, we choose $f_1 = 17$ GHz and $f_2 = 27$ GHz as working frequencies for the cost function [see Equation (1)].

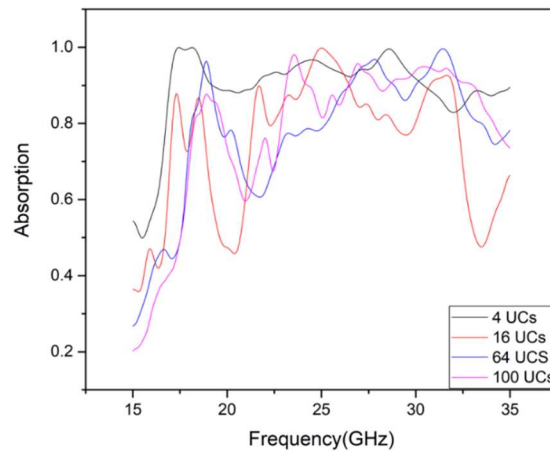


Figure 2. Absorptivity curves of random metamaterial absorbers with 4, 16, 64, 100 UCs

Figure 3 shows the absorption spectrum of 2×2 and 3×3 UCs structures using the GA method. The GA produces identical results to those obtained by the traditional methods in Ref. [46]. In this article, to prove our structure's advanced property, we have compared the bestfit structure with the structure obtained by the traditional methods in reference [46]. Specifically, the structure by CFM (combination of fundamental meta-block) method. MB stands for meta-block, a set of basic blocks with the number of UC greater than 1. And MB3x3, MB4x4 are the meta-blocks with 3×3 , 4×4 UCs while the last number (for example MB3x3-1) indicates the specific configuration from the other cases. The absorption spectra of the final configuration (labeled as 'bestfit') in both cases are mostly higher than 90% throughout the frequency band of interest. However, the absorption spectrum of the 2×2 bestfit configuration is not stable. This is caused by the limitation of possibilities in this case. The total number of possibilities in the population is only 16 ($= 2^{2 \times 2}$), hence the GA does not have enough samples to mutate and optimize.

For the structures consist of 4x4, 5x5, 6x6 UCs, or higher, the number of possible random configurations can become enormous. For example, the number of 4x4 UCs random configurations is in order of $2^{4 \times 4} = 2^{16} = 65536$, of 5x5 UCs configurations is 33,554,432. As a result, the computational cost for random samples is extremely large. Figure 4 (A) displays the simulation results of 4×4 UCs structure based on GA by setting the initial population to be 30 configurations and the maximum number of iteration to be 20 generations. Shown are the absorption spectrum at several generations (iga = 0, 8, 16 and 19) and at number index of each corresponding generation (ip = 2, 3, 4, 5, 6). It can be seen that the absorption curve “4 x 4 GA Bestfit” achieved after 20 generations show the broadband range with the highest absorption, indicating the validity in our approach. Note also that at lower numbers of generations, the absorption value may fluctuate at $\sim 90\%$ throughout the GA simulation and is not always improved through generations. Since the process of GA methods is based on natural selection, we normally expect the offsprings to have better absorption spectra than the parents from the previous generations. However, to diversify the new generation, numerous offsprings are selected and some mutations are added to the gene pool. This process is governed by the crossover and mutation which are mostly random. In detail, for the crossover session, the parents’ samples are paired up with the crossovers probability P_{cross} . The crossover can happen at one or more points between more than one chromosome. After the crossover process, random mutations will be applied to the samples with the mutation probability P_{mut} . On this process, random bits of the binary matrix will be reversed. For example, when the mutation occurs on the fifth bit of the binary string {11111} it will be mutated to the binary string {11110}. This may lead to the fact the next generation may have lower fitness and absorption spectra than the previous ones. But, considering the whole process, the final result (bestfit structure) always has the best absorption spectrum. Moreover, a comparison of the current result to our previous one in [16] shows a significant improvement in the average absorption values.

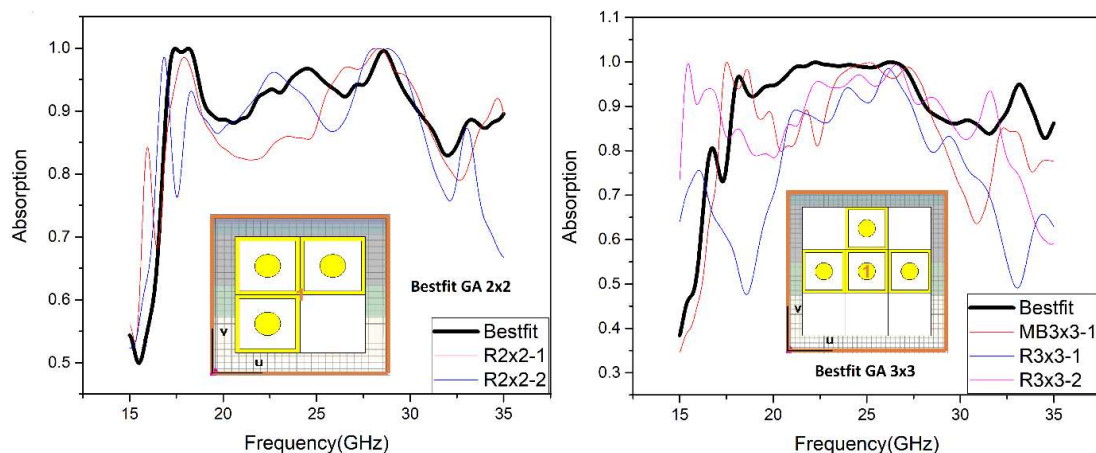


Figure 3. The absorption spectra of full-sized absorbers optimized by GA with the size of 2x2 and 3x3 UCs compare to other configurations created by the traditional methods

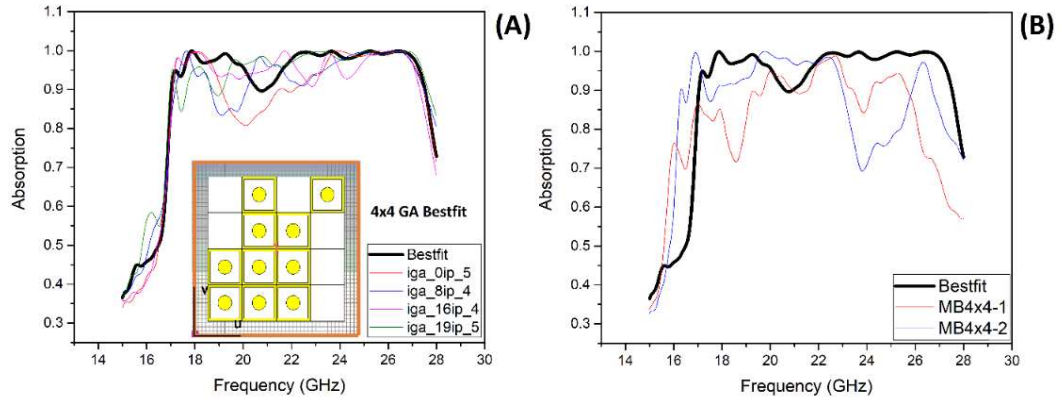


Figure 4. The absorption spectrum of full-sized absorbers structure with 4x4 UCs optimized by GA compares to (A) other configurations created in some particular generations, (B) other configurations generated by traditional methods

A similar trend can be also observed for 5x5 and 6x6 UC structures (Figure 5).

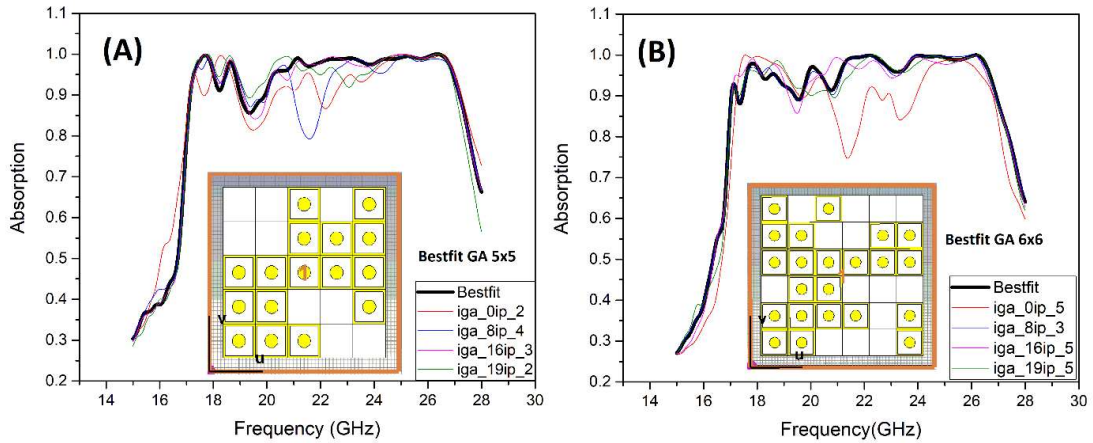


Figure 5. The absorption spectrum of full-sized absorbers optimized by GA compare to other configurations created in some generation with the number of UCs: (A) 5x5, (B) 6x6

Similar to the 4×4 UCs case, the absorption curves in these cases are also not improved gradually throughout the generations but the bestfit's figure is very stable and remains more than 90% throughout the working frequency band.

In this article, we have set the same initial population (30) and the maximum number of iteration (20) for the structures from 4x4 UCs to 6x6 UCs. It is quite clear that the 4x4 UCs' result is better than the other two. Hence, we may predict that when the initial values are the same, the structure with a smaller size can have a better absorption spectrum because of the total number of configurations evaluated by the GA can cover a larger percentage over the set of total possible configurations. We will study more about this issue in our future project by comparing the absorption spectra of the structures with the same number of UCs but generated with different initial population and the maximum number of iteration.

3. Conclusions

In summary, we present a novel way to approach coding metamaterial absorbers by using a GA route. By using the GA, 5 configurations with different numbers of UCs (namely 2×2 , 3×3 , 4×4 , 5×5 , and 6×6 UCs) have been generated and they all have absorption spectra remaining mostly higher than 90% throughout the frequency band of interest. Additionally, the process of the research is simpler and more flexible when studying numerous structures with various number of UCs since GA only requires one step of input the desired number of UCs and can work automatically. This result has proven the outstanding advantages of the GA method and paved a new approach to design perfect coding metamaterial absorbers.

REFERENCES

- [1] Diem, M., Koschny T., Soukoulis, C. M., 2009. Wide-Angle Perfect Absorber/Thermal Emitter in the Terahertz Regime. *Phys. Rev. B* **79**, 033101.
- [2] Bossard, J. A., Werner, D. H. 2013. Metamaterials with Angle Selective Emissivity in the Near-Infrared. *Opt. Express*, **21**, 5215-5225.
- [3] Bossard, J. A.; Werner, 2013. D. H. Metamaterials with Custom Emissivity Polarization in the Near-Infrared. *Opt. Express*, **21**, 3872-3884.
- [4] Liu, X., Tyler, T., Starr, T., Starr, A. F., 2011. Jokerst, N. M.; Padilla, W. J. Taming the Blackbody with Infrared Metamaterials as Selective Thermal Emitters. *Phys. Rev. Lett.*, **107**, 045901.
- [5] Engheta, N. and Ziolkowski, R. W., 2006. *Metamaterials: Physics and Engineering Explorations*, Wiley-IEEE Press.
- [6] Tran, C.-M. et al., 2010. High impedance surfaces based antennas for high data rate communications at 40 GHz. *Prog. Electromagn. Res.* **13**, 217-229.
- [7] Kundtz, N. & Smith, D. R., 2010. Extreme-angle broadband metamaterial lens. *Nat. Mater.* **9**, 129-132.
- [8] Landy, N. I., Bingham, C. M., Tyler, T., Jokerst, N., Smith, D. R., Padilla, W. J., 2009. Design, Theory, and Measurement of Polarization-Insensitive Absorber for Terahertz Imaging. *Phys. Rev. B* **79**, 125104.
- [9] Diem, M., Koschny, T., Soukoulis, C. M., 2009. Wide-Angle Perfect Absorber/Thermal Emitter in the Terahertz Regime. *Phys. Rev. B* **79**, 033101.
- [10] Wang, C., Yu, S., Chen, W., Sun, C., 2013. Highly Efficient Light- Trapping Structure Design Inspired by Natural Evolution. *Sci. Rep.* **3**, 1025.
- [11] Teperik, T. V., García de Abajo, F. J., Borisov, A. G., Abdelsalam, M., Bartlett, P. N., Sugawara, Y., Boumberg, J. J. Omni, 2008. Directional Absorption in Nanostructured Metal Surfaces. *Nat. Photonics*, **2**, 299-301.
- [12] Hibbins, A. P., Murray, W. A., Tyler, J., Wedge, S., Barnes, W. L., Sambles, J. R., 2006. Resonant Absorption of Electromagnetic Fields by Surface Plasmons Buried in a Multilayered, *Phys. Rev. B* **74**, 073408.
- [13] Bossard, J. A.; Werner, D. H., 2013. Metamaterials with Custom Emissivity Polarization in the Near-Infrared. *Opt. Express*, **21**, 3872-3884.

- [14] Veselago, V. G., 1968. The electrodynamics of substances with simultaneously negative values of ϵ and μ . *Sov. Phys. Usp.*, **105**, 509.
- [15] Watts, C. M., Liu, X. & Padilla, W. J., 2012. Metamaterial Electromagnetic Wave Absorbers. *Adv. Mater.*, **24**, 23.
- [16] Cuong, T. M.; Hai P. V.; Hung H. T.; Thuy N. T., Tung D. H., Khuyen B. X., Tung B. S.; Tuyen L. D., Linh P. T. & Lam V. D., 2020. Broadband microwave coding metamaterial absorber. *Sci. Rep.* **10**, 1810.
- [17] Hao, J. M. et al., 2010. High performance optical absorber based on a plasmonic metamaterial. *Appl. Phys. Lett.*, **96**, 251104.
- [18] Cuong, T. M. et al., 2019. Creating Multiband and Broadband Metamaterial Absorber by Multiporous Square Layer Structure. *Plasmonics*, <https://doi.org/10.1007/s11468-019-00953-6>.
- [19] Gong, C. et al., 2016. Broadband terahertz metamaterial absorber based on sectional asymmetric structures. *Sci. Rep.*, **6**, 32466.
- [20] Kenney, Metal, 2017. Octave-Spanning Broadband Absorption of Terahertz Light Using Metasurface Fractal-Cross. *ACS Photonics* **4** (10), 2604.
- [21] Chen, K. et al., 2016. Broadband microwave metamaterial absorber made of randomly distributed metallic loops, IMWS-AMP, 7588420. <https://doi.org/10.1109/IMWS-AMP.2016.7588420>.
- [22] Peng, Y. et al., 2019. Broadband Metamaterial Absorbers. *Opt. Mater* **7**, 1800995.
- [23] Lobet, M., Lard, M., Sarrazin, M., Deparis, O. & Henrard, L., 2014. Plasmon hybridization in pyramidal metamaterials: a route towards ultra-broadband absorption. *Opt. Express*, **22**, 12678.
- [24] Xin, W., Binzhen, Z., Wanjun, W., Junlin, W. & Junping, D., 2017. Fabrication and Characterization of a Flexible Dual-band Metamaterial Absorber. *IEEE Photonics J.*, **9**, 4600213.
- [25] Tao, H. et al., 2008. Highly exible wide angle of incident terahertz metamaterial absorber: Design, fabrication, and characterization. *Phys. Rev. B* **78**(24), 241103.
- [26] Mattiucci et al., 2013. Impedance matched thin metamaterials make metals absorbing. *Sci. Rep.*, **3**, 3203, <https://doi.org/10.1038/srep03203>.
- [27] Zheludev, N. I. & Eric, P., 2016. Recon gurable nanomechanical photonic metamaterials. *Nat. Nanotech.*, **11**, 16.
- [28] Xiong, X. et al., 2013. Structured Metal Film as a Perfect Absorber. *Adv. Mater.*, **25**, 3994, <https://doi.org/10.1002/adma.201300223>.
- [29] Liu, C. & Qi, L. and Mingjing, 2018. Broadband infrared metamaterial absorber with polarization-independent and wide-angle absorption. *Opt. Mater. Express*, **8**, 82439.
- [30] Cuong, T. M., Thuy, N. T. & Tuan, L. A., 2016. Influence of Structural Parameters on a Novel Metamaterial Absorber Structure at K-band Frequency. *J. Electron. Mater.*, **45**(5), 2591-2596.